Journal of Renewable Materials

Tech Science Press

DOI: 10.32604/jrm.2022.024994

check for updates

ARTICLE

Effect of Natural Zeolite on Pore Structure of Cemented Uranium Tailings Backfill

Fulin Wang*, Xinyang Geng, Zhengping Yuan and Shijiao Yang*

School of Resource & Environment and Safety Engineering, University of South China, Hengyang, 421001, China

*Corresponding Authors: Fulin Wang. Email: wangfl2009@126.com; Shijiao Yang. Email: cute1088@sina.com

Received: 16 June 2022 Accepted: 27 July 2022

ABSTRACT

The use of some environmental functional minerals as backfill-modified materials may improve the leaching resistance of cemented uranium tailings backfill created from alkali-activated slag (CUTB), but these materials may participate in the hydration reaction of the cementitious materials, which could have a certain impact on the pore structure of the CUTB, thus affecting its mechanical properties and leaching resistance. In this paper, natural zeolite is selected as the backfill-modified material, and it is added to alkali-activated slag paste (AASP) and CUTB in cementitious material proportions of 4%, 8%, 12%, and 16% to prepare AASP mixtures and CUTB mixtures containing environmental functional minerals. After the addition of natural zeolite, the porosity of the CUTB generally increases, but when the content is 4%, the porosity decreases to 22.30%. The uniaxial compressive strength (UCS) of the CUTB generally decreases, but the decrease is the smallest when the content is 4%, and the UCS is 12.37 MPa. The addition of natural zeolite mainly reduces the number of fine pores in the CUTB, but the pores with relaxation times T_2 of greater than 10 ms account for about 10% of the total pores, and there are a certain number of large pores in the CUTB. The main product of alkali-activated slag is calcium (alumino)silicate hydrate (C-(A)-S-H gel). When natural zeolite is added, the hydration products develop towards denser products with a high degree of polymerization and the formation of low polymerization products is reduced. This affects the internal fracture pores of the hydration products and the interface pores of the CUTB, has an irregular effect on the pore characteristics of the CUTB, and influences the UCS.

KEYWORDS

Pore structure; cemented backfill; natural zeolite; uranium tailings; LF-NMR

Nomenclature

CUTB	Cemented uranium tailings backfill created from alkali-activated slag
AASP	Alkali-activated slag paste
UCS	Uniaxial compressive strength
C-(A)-S-H	Calcium (alumino)silicate hydrate
LF-NMR	Low field nuclear magnetic resonance
SEM	Scanning electron microscope
FTIR	Fourier transform infrared spectrometer
NMR	Nuclear magnetic resonance

1 Introduction

The cement solidification/stabilization technique is an important method for the disposal of medium and low-level radioactive waste, and it is also one of the earliest mature methods for industrial application [1,2]. However, it is obviously inappropriate to completely rely on the process of cement solidification disposal of medium and low-level radioactive waste for large volumes of low (extremely low) radioactive solid waste such as uranium tailings. In recent years, the development of the paste backfill technique and its new cementitious materials have provided important ideas and references for the disposal of uranium tailings based on the principle of cement solidification [3–5]. Uranium tailings are different from the medium and low-level radioactive waste discharged by nuclear power plants. They are solid waste from various sources and are discharged during uranium resource mining, beneficiation, and metallurgy. Although their volume is often relatively large, the content of radionuclides is extremely low. If the underground cemented backfill treatment of uranium tailings is adopted, it does not need to be as high as the cement solidified body of medium and low-level radioactive waste, and it only needs to be higher than the treatment standard for uranium tailings stored on the surface. In addition, cemented backfill of uranium tailings is different from traditional cemented backfill. Its main quality index is no longer the compressive strength, and it must have a good leaching resistance on the premise of a certain compressive strength [6,7]. The high leaching rate of radionuclides is a deficiency of cement solidified medium and low-level radioactive waste, which also reminds us that we should pay close attention to the leaching resistance if the cemented uranium tailings backfill created from alkali-activated slag CUTB method is adopted.

Uranium tailings are produced by a wide range of sources, mainly including heap leaching tailings, hydrometallurgical tailings, drilling mud, and mining waste rock. Uranium tailings from various sources have a wide range of particle size distributions, from clay to gravel. Moreover, due to the different leaching processes, the elements contained in the uranium tailings are also very complex. These factors directly affect the hydration reaction, pore structure, permeability, and compactness of the CUTB and thus affect its mechanical properties and leaching resistance. Numerous studies conducted by experts and scholars have shown that the complex physics and chemistry of uranium tailings affect the performance of cemented backfill, which restricts its use as aggregate in filling engineering applications [8–12]. Recently, many experts and scholars have paid a great deal of attention to smelting slag as a substitute for backfill cementitious materials. This type of new cementitious materials, represented by alkali-activated slag, has a low cost, and these materials generally have the advantages of good water retention, corrosion resistance, and high later strength. Zhang et al. demonstrated that the use of smelting slag can solve the problems of expansion, strength reduction, and even disintegration of high sulfur tailings aggregate filling bodies [13–17]. This indicates that if alkali-activated slag is used as the cementitious material, it should be possible to solve the problems of the poor mechanical properties and poor long-term stability of CUTB and thus to improve its leaching resistance to a certain extent.

In backfill mining, in order to improve the fluidity of the filling slurry and the mechanical properties of the filling body, a certain quantity of backfill-modified materials is usually added [18–20]. For the cemented uranium tailings backfill created from alkali-activated slag cementitious materials, in addition to its mechanical properties, we should pay more attention to its leaching resistance [21–23]. If appropriate materials are added to improve the leaching resistance of the CUTB, such materials also fall into the category of backfill-modified materials. Krajnak et al. [24–26] reported that natural zeolite, an environmental functional mineral with a good adsorption and exchange capacity, also has a good uranium adsorption capacity. However, the mineral composition of these materials is basically consistent with the slag used to prepare cementitious materials. The environmental functional minerals added should participate in the formation of hydration products. Most studies have shown that the addition of these materials has a positive effect on the formation of hydration products; however, after these functional minerals are added, the strengths of the alkali-activated slag cementitious materials and its mortar or

concrete are weakened to a certain extent. In the underground cemented backfill treatment of uranium tailings, we have to consider the coordination of the weakening and strengthening effects on the filling structure and leaching resistance.

When natural zeolite is added as the modified material of CUTB, it is of positive significance to further study the mechanical properties and leaching resistance by exploring its influence on the pore structure of CUTB. To explore the influence of natural zeolite on the pore structure of CUTB, we also need to discuss the influence of the polymerization degree of hydration products on the formation of pore structure from the perspective of the hydration products of alkali-activated slag mixed with natural zeolite, and discuss and analyze the types and formation mechanism of the pore structure in the filling body from the perspective of the physical and chemical processes of slurry mixing, pouring, forming, and curing.

2 Materials and Methods

2.1 Experimental Materials

The experimental materials included the backfill aggregates, cementitious materials, and modified materials.

(1) The backfill aggregate selected for the experiments was hydrometallurgical tailings stacked in a tailings pond, with a water content of 10.91% and a density of 2.55 t/m^3. The results of the particle size screening revealed that the inhomogeneity coefficient was 2.31, the curvature coefficient was 0.93, the grain size distribution of the tailings was discontinuous and non-uniform, and the gradation was not good.

(2) The cementitious material selected for the experiments was alkali-activated slag. The slag was S95 granulated blast furnace slag micropowder produced by a building materials enterprise. Its specific surface area was 431 m^2/kg, its chemical modulus was $K = 1.91$, its alkali modulus was $Mo = 0.97$, and its activity coefficient was $Ma = 0.52$. The activator was sodium silicate, and its modulus was adjusted to 1.2 using NaOH.

(3) The modified material selected for the experiments was mainly natural zeolite. Its silicon to aluminum ratio k was 5.22, making it a medium silica zeolite (Table 1). In addition, CL90-QP grade Quicklime powder was selected as the auxiliary material, and urban tap water was directly selected as the water for the experiments.

Table 1: Main chemical compositions of modified materials

	SiO_2	Al_2O_3	K_2O	Na_2O	CaO	MgO	Fe_2O_3	TiO_2	Cl^-	MnO	SO_3	P_2O_5
Natural zeolite	74.990	14.360	4.461	2.736	1.342	0.987	0.819	0.128	0.061	0.052	0.029	0.013
Quicklime	1.240	0.540	0.070	0.351	94.780	2.310	0.411	0.036	——	0.006	——	0.009

2.2 Experimental Plan

To explore the influence of natural zeolite on the pore structure of CUTB, it was necessary to analyze the distribution characteristics of the pore structure and the formation of the hydration products. To avoid the adverse effect of the uranium tailings mixed in the materials during the analysis and sampling of the hydration products on the test results, two types of experiments were designed for the CUTB and AASP.

1) **Experiments on CUTB.** To explore the influence of the addition of functional minerals on the pore structure of CUTB, the following experimental parameters were fixed. The filling slurry was prepared with a water to solid ratio of 0.25 and a cement to sand ratio of 1:4. The modulus of the sodium silicate in the activator was 1.2, and the alkali equivalent of Na_2O accounted for 6% of the mass ratio of the cementitious materials. Quicklime powder was added as an auxiliary

material, accounting for 6% of the cementitious materials. The natural zeolite was mixed into the filler in proportions of 4%, 8%, 12%, and 16% of the cementitious materials for comprehensive testing (Table 2). For comparison, a control group with no functional minerals added (i.e., 0%) was also prepared.

2) **Experiment on AASP.** To explore the characteristics of the hydration products of the AASP when natural zeolite was added, only the maximum content of natural zeolite in the above experiments was used to study the characteristics of the hydration products under the specific water to solid ratio and the addition of activator. That is, granulated blast furnace slag was selected as the base material of the cementitious materials, sodium silicate was used as the activator, the fixed alkali equivalent was 6%, the modulus was 1.2, the water to solid ratio was 0.4, and the content of natural zeolite was 16%. A control group with no functional minerals added (i.e., 0%) was also prepared (Table 3).

Table 2: Experimental design of CUTB

No.	Natural zeolite addition	Quicklime powder addition	Alkali equivalent of Na_2O	Activator modulus	Cement to sand ratio	Water to solid ratio
1	0%					
2	4%					
3	8%	6%	6%	1.2	1:4	0.25
4	12%					
5	16%					

Table 3: Experimental design of AASP

No.	Natural zeolite addition	Alkali equivalent of Na_2O	Activator modulus	Water to solid ratio
1	0%	6%	1.2	0.40
2	16%			

2.3 Experimental Scheme

The pore structure and its distribution are one of the factors controlling the strength of CUTB. In the radioactive waste cement solidification system, the leaching resistance is directly or indirectly affected by the physical and chemical seepage. By measuring the relaxation time of the fluid in the pore structure of the filling body using low field nuclear magnetic resonance (LF-NMR), we obtained its internal pore distribution, connectivity characteristics, and various physical parameters for a qualitative and quantitative analysis of the internal pore distribution. Due to the short testing time and non-destructive characteristics of LF-NMR, it is one of the most effective methods of analyzing the pore structure of a filling body.

1) **Preparation of CUTB.** First, according to the proportion designated in the experimental plan and the Standard for test methods of performance of building mortar (JGJ/T70-2009), the filling materials were mechanically mixed using a JJ-5 cement mortar mixer. During the mixing, the materials were mixed at low speed for 120 s, then suspended for 15 s, and then mixed at high-speed for 120 s to ensure that all of the materials were evenly mixed. Then, the prepared slurry was poured into Φ50 mm × 50 mm cylindrical molds, and the samples were vibrated manually to eliminate bubbles formed during the pouring of the material into the mold. Finally, the cast sample was placed in a curing box (25 ± 5°C, humidity ≥ 95%). It was removed from the mold after 24 h and allowed to continue curing for an additional 27 days (i.e., a total of 28 days of curing).

2) **LF-NMR analysis.** First, the uniaxial compressive strength (UCS) test was carried out on the filling specimen cured for 28 days. Second, the filling specimens were saturated with water, and the water on the surface of the filling specimen was wiped away. Then, the filling samples were tested using an AniMR-150 rock magnetic resonance imaging analysis system, and the porosity and relaxation time T_2 distribution characteristics of the CUTB were obtained.
3) **Analyses of microstructure and hydration products of CUTB.** First, a group of filling specimens with natural zeolite contents of 0% and 16% were selected for analysis. Second, these specimens were broken, the fresh fracture surfaces were collected for analysis, and the microstructure was observed using a MERLIN Compac 60–95 scanning electron microscope. Third, the hydration products in the broken filling body were screened and analyzed via Fourier infrared spectroscopy (FTIR) using a Nicolet 380 Fourier transform infrared spectrometer. In addition, NMR analysis of ^{29}Si and ^{27}Al was conducted using an AVANCE NEO 600M solid-state NMR spectrometer.
4) **Analysis of hydration products of AASP.** First, the consolidated body of AASP was crushed and sieved. Then, as with the CUTB, SEM, FTIR, and NMR analyses were carried out.

3 Results and Discussion

3.1 T_2 Distribution Characteristics

The pore size of the CUTB was positively correlated with the relaxation time T_2, that is, the change in T_2 reflected the change in the pore size in the sample. A larger T_2 value indicates a larger pore radius, and vis versa. The transverse relaxation time T_2 and the peak relaxation time area can reflect the size and number of pores in the sample [27,28].

For all of the natural zeolite contents, there was one main peak and several secondary peaks on the T_2 diagram of the CUTB (Figs. 1 and 2). Since different T_2 values represent different pore sizes, if the T_2 value at the inflection point of the curve on the T_2 diagram is taken as the boundary value, the T_2 diagram can be divided into several zones. The enclosed area of each zone is the porosity of the corresponding range. The T_2 diagram for the CUTB with natural zeolite contents of 0%–16% was divided into five zones, but the boundaries between two adjacent zones on some diagrams were not very clear, and they could be combined into one zone. For example, the boundary between zones III and IV on the diagram was not very clear for the CUTB with a natural zeolite content of 0% (Fig. 1). It should be noted that the boundary value for dividing two zones was not the same for the T_2 diagrams of the different filling samples.

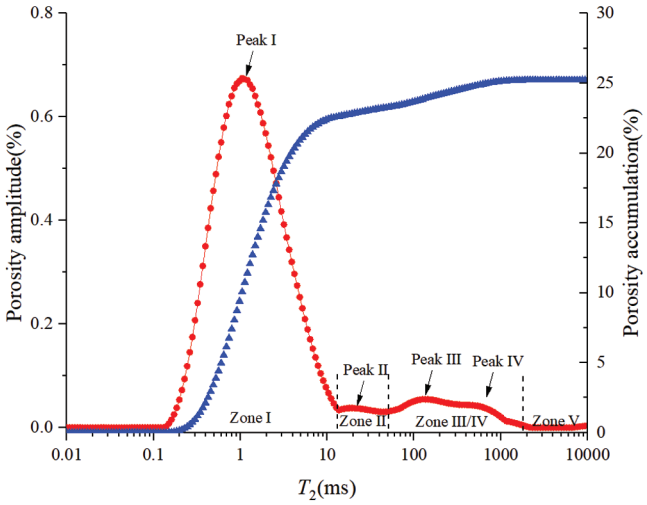

Figure 1: T_2 diagram for the CUTB with a natural zeolite content of 0%

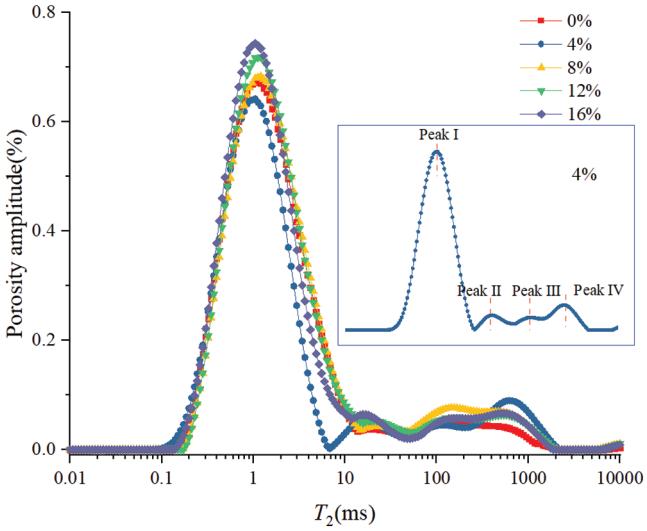

Figure 2: T_2 diagram for the CUTB with different natural zeolite contents

On the T_2 diagram of the CUTB mixed with natural zeolite, the characteristics of the relaxation peaks were more obvious. In particular, when the zeolite content was 4%, there were four obvious characteristic peaks (mini diagram in Fig. 2). However, the test results of the three groups with natural zeolite contents of 8%, 12%, and 16% show that the boundary between the third and fourth characteristic peaks was not obvious. After adding natural zeolite, the first characteristic peak of the T_2 diagram of the CUTB shifted to the left compared with that without the addition of natural zeolite; and its relaxation time range (i.e., the range of zone I) was significantly narrower, which indicates that after adding natural zeolite, the small pores in the CUTB are significantly reduced. In particular, when the natural zeolite content was 4%, not only did the range of zone I narrow, i.e., 0.080–6.826 ms, but the peak value of the first peak (the relaxation time represents the proportion of pores with corresponding size) was also significantly reduced compared with the other groups. In the group of samples with a natural zeolite content of 4%, the total number of pores was only 22.30%, which was much lower than those of the other groups. The proportion of zone I was 83.13%, and the proportion below 10 ms was 83.50% (Table 4). As the natural zeolite content continued to increase from 8% to 16%, the total number of pores in the CUTB initially increased and then decreased, reaching the maximum value when the content was 12%, and the proportion of the zone of the first relaxation peak also exhibited the same trend. This also shows that when an appropriate amount of natural zeolite is added, the porosity of the CUTB can be reduced, especially the proportion of fine pores.

In addition to the division determined according to the minimum value for the proportion of component with different relaxation times as the limiting value, zone V generally appeared in all of the test results. This zone is characterized by large pores due to the large relaxation time. This may be due to the insufficient drying of the surface of the specimen containing free water, or it may be due to the large pores caused by bubbles in the surrounding wall of the specimen (Fig. 3).

3.2 Micromorphology

To further verify the pore characteristics of the CUTB from the perspective of the micromorphology, the fracture surface of the CUTB was scanned via SEM (Fig. 4). No obvious needle-like and flake-like features were observed on the fracture surface of the CUTB, which are mainly accumulations formed by granular disorderly connections, as well as flocs formed via fibrous agglomeration. These products form a dense structure. It can be inferred that the hydration products may be mainly calcium aluminosilicate hydrate

(C-A-S-H) or calcium silicate hydrate (C-S-H) and other amorphous calcium (alumino)silicate hydrate (C-(A)-S-H) materials. The dense structure of the hydration products should theoretically cause the filling body formed to have smaller pores and a higher strength.

Table 4: Relaxation time partitions of the T_2 diagrams and the porosity ratio

Natural zeolite content	T_2 (ms)					Porosity (%)				
	Zone I	Zone II	Zone III	Zone IV	Zone V	Zone I	Zone II	Zone III	Zone IV	Zone V
0%	0.139–13.667	13.667–44.488	44.488–2171.118		2171.118–10000	89.71	2.28	7.96		0.05
4%	0.080–6.826	6.826–47.686	47.686–204.907	204.907–2327.202	2327.202–10000	83.13	4.38	3.62	8.74	0.13
8%	0.172–14.650	14.650–47.686	47.686–333.129	333.129–2171.118	2171.118–10000	85.90	2.57	6.84	4.51	0.18
12%	0.185–15.703	15.703–51.114	51.114–252.354	252.354–2025.502	2025.502–10000	87.53	2.80	4.38	5.11	0.18
16%	0.150–11.895	11.895–51.114	51.114–235.429	235.429–1889.652	1889.652–10000	87.05	3.49	3.87	5.45	0.14

(a) Appearance of surface of CUTB (b) Internal fracture surface of CUTB

Figure 3: Apparent pore characteristics of CUTB

However, from the SEM images of the fracture surface of the CUTB with a magnification of 200 times, it can be seen that there are a large number of circular or irregular pore structures in addition to the circular pit like holes formed at the interface between the uranium tailings and the hydration products. When magnified to 1,000 times, fine cracks were also observed. When further magnified to 5,000 times, these cracks were clearly visible. When magnified to 10,000 times, it was found that in addition to these fractures, there were very small pores.

To eliminate the influence of the pore structure of the hydration products themselves, the AASP with the same amount of natural zeolite was observed using SEM (Fig. 5). No obvious circular or irregular pore structures were observed. That is, these pore structures only existed in the CUTB with uranium tailings added as the aggregate. It can also be seen from Fig. 3 that in addition to the internal fracture surface of the CUTB, the surface of the CUTB also contained visible pore structures. This explains why zone V appears on the T_2 diagrams.

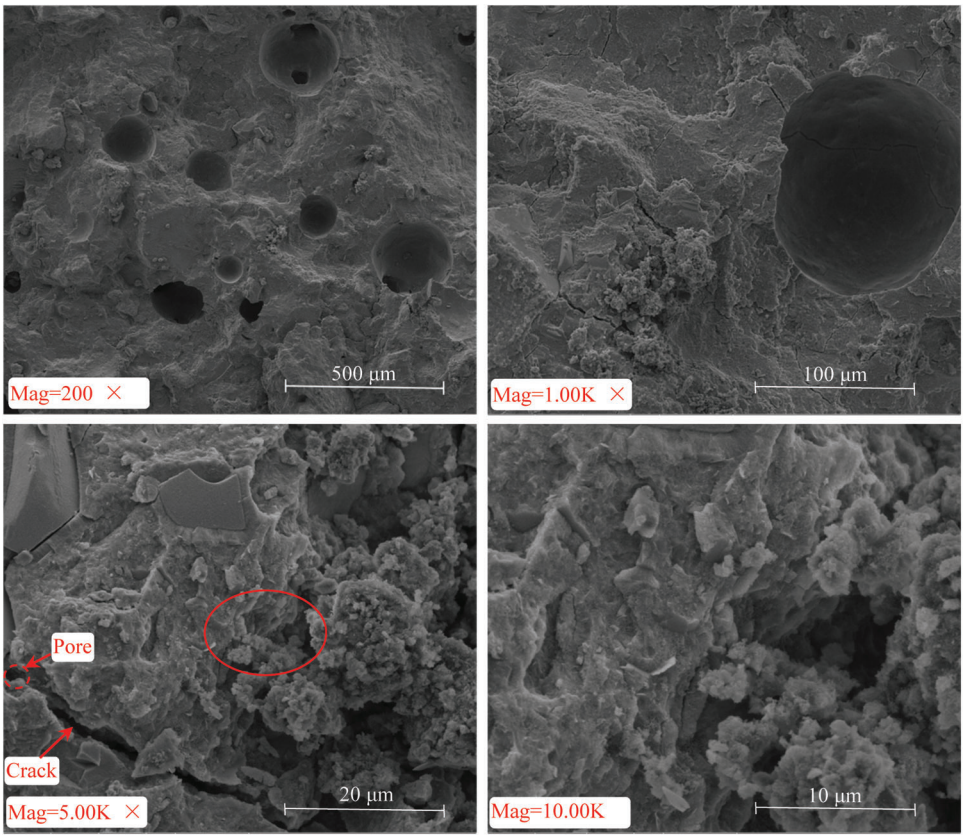

Figure 4: SEM scanning image of CUTB mixed with natural zeolite

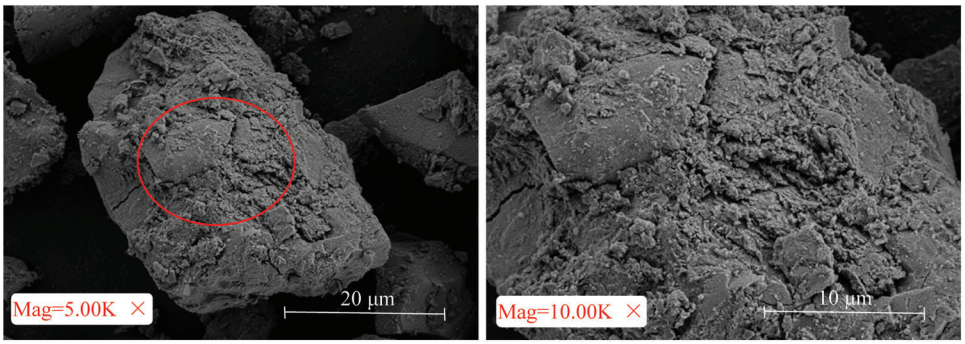

Figure 5: SEM images of AASP mixed with natural zeolite

The reaction of the filling slurry containing cementitious material to form the filling body is a three-phase dynamic adjustment process involving solid, liquid, and gas. In addition to free water, capillary water, and adsorbed water, there are gas or bubble attachments in the stirred filling slurry. During the alkali-activated slag reaction, the space occupied by the water molecules and gas is gradually occupied by the generated hydration products, which makes the filling body denser and increases its strength. Moreover, some of space is not effectively filled, resulting in the formation of the pore structure of the filling body. Only from the perspective of space occupation, the products with a low degree of polymerization are more conducive to diffusion into these spaces. However, when an appropriate amount

of natural zeolite is added, because the structure of the zeolite is more compact and the proportion of fine pores is reduced, the total pore space in the filling body is greatly reduced.

For the filling body containing uranium tailings with alkali-activated slag as the cementitious material, whether natural zeolite is added or not, the pore structure can be divided into interfacial pores and the internal cracks and pores in the hydration products. The interfacial pores include the pores between the interfaces of the filling aggregate and hydration products, between the filling aggregate and filling aggregate, and between the hydration products and hydration products, which are based on the particle size composition of the uranium tailings as the filling aggregate. The bubbles generated during the mixing and molding of the slurry and the properties of the alkali-activated slag cementitious material affect the generation of the interfacial pores.

3.3 Relationship between Porosity and UCS

In theory, the larger the porosity of the CUTB is, the worse its uniaxial compressive strength (UCS) and other mechanical properties are. The porosity and UCS of the CUTB samples with different natural zeolite contents were analyzed to investigate the correlations between the properties (Fig. 6). There was no obvious functional relationship between the UCS and porosity of the CUTB, but there was a certain trend between them, that is, the UCS of the CUTB decreased with increasing porosity, which is similar to the general law of the UCS of rocks and rock-like concrete samples with porosity. It should be noted that the fitting degree of the trend line between the two was very low. In particular, when the natural zeolite content was 0%–16%, the R^2 value was only 0.388, and the p-value was 0.262, indicating that the fitting effect was not significant at this time. The main reason for this is that when the natural zeolite content was 0%, although the porosity of the CUTB was relatively large, its UCS was still the maximum for the test group. When the natural zeolite content was 4%, although the porosity of the CUTB was greatly reduced, its UCS was also reduced to a certain extent.

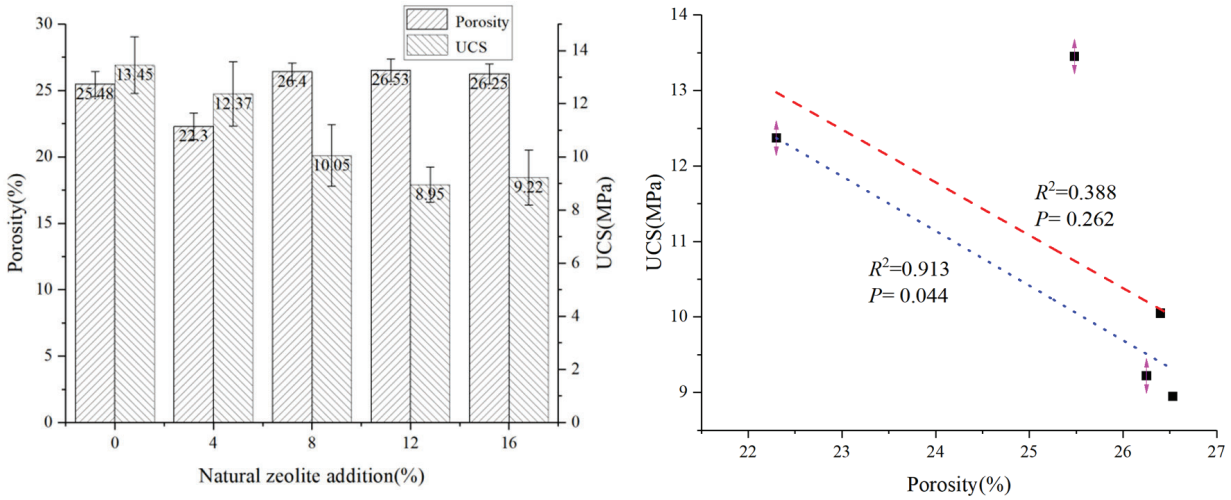

(a) Variations in the UCS and porosity of the CUTB containing natural zeolite

(b) Relationship between the UCS and porosity of the CUTB

Figure 6: Correlation between the porosity and UCS of the CUTB

There was no exact functional relationship between the UCS of the CUTB and its porosity, which further shows that the formation of the mechanical properties of the CUTB was very complex when natural zeolite was added as the backfill-modified material. The mechanical properties of the CUTB were not only related to

the pore structure but also to the hydration products of the alkali-activated slag mixed with the natural zeolite, which in turn affected the formation of the pore structure. In addition, after adding natural zeolite, the fluidity of the uranium tailings filling the slurry also changed, which also affected the formation of the interfacial pores in the CUTB due to improper vibration when the slurry was poured into the molds. Therefore, it was necessary to analyze the hydration products of the alkali-activated slag mixed with the natural zeolite.

3.4 FTIR Analysis of Hydration Products

The molecular structure and degree of polymerization of the alkali-activated slag hydration products were characterized by analyzing the characteristic peaks of the FTIR spectra (Fig. 7).

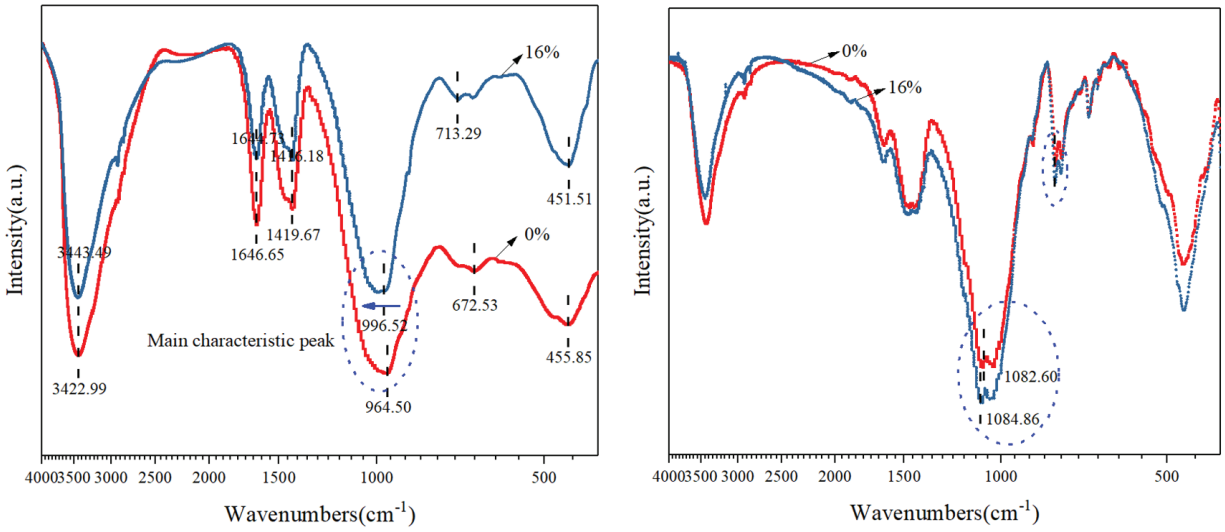

(a) FTIR spectra of the AASP hydration products

(b) FTIR spectra of the hydration products in the CUTB

Figure 7: FTIR spectra of the hydration products

In the FTIR spectrum of the hydration products of the AASP with a natural zeolite content of 0%, the main characteristic peak was located at 964.50 cm^{-1}. Shi et al. [29–32] reported that the main cementing components of geopolymer and alkali-activated slag may be C-A-S-H or sodium aluminosilicate hydrate (N-A-S-H), and the 960–970 cm^{-1} peak is generally ascribed to the asymmetric stretching vibration of Si-O in hydrated calcium silicate hydrate, and the calcium ions promote the formation of a C-(A)-S-H structure. According to the main characteristic peaks in the spectrum and the chemical composition of the slag materials, it was concluded that the hydration products were mainly C-(A)-S-H gels. It can be seen from the T-O-T wave number corresponding to SiQ^n (where n values of 4, 3, 2, 1, and 0 correspond to 1200, 1100, 1000, 900, and 850 cm^{-1}, respectively) that the silica tetrahedron in the hydration products of the AASP was mainly Q^2.

In the FTIR spectrum of the hydration products of the AASP with a natural zeolite content of 16%, the main characteristic peak in the range of 800–1300 cm^{-1} shifted to 996.52 cm^{-1} (i.e., toward a high wave number), which is closer to the wave number of 1000 cm^{-1} corresponding to Q^2. This indicates that the hydration products were still mainly Q^2, but the natural zeolite participated in the alkali-activated slag reaction, and the hydration products had a higher degree of polymerization. The absorption peak at 713.29 cm^{-1} is caused by the substitution of Al for Si in the Si-O tetrahedra tetrahedron and the formation of Si-O-Al bonds, which further indicates that the hydration products were mainly C-(A)-S-H gels.

Compared with the hydration products of the AASP, in the FTIR spectrum of the hydration products in the CUTB, each characteristic peak shifted in the higher wave number direction to a certain extent. When 0% and 16% natural zeolite were added, the main characteristic peaks were located at 1082.60 cm^{-1} and 1084.86 cm^{-1}, respectively, which were generated by the asymmetric vibration of the Si-O-T (where T represents Si or Al) structure. When the Al content of the structure increases, the peak shifts in the lower wave number direction. The characteristic peak observed in the spectra is also a sign of the hydration products of the AASP. The absorption peaks at 789.25 cm^{-1} and 778.16 cm^{-1} are due to the symmetrical stretching vibration of Si-O-Si, but these two characteristic peaks were not observed in the hydration products of the AASP, which may be due to the uranium tailings mixed in the sample.

It can be seen that when natural zeolite was added, the hydration products had a higher degree of polymerization. In the backfill system, the use of uranium tailings as the filling aggregate had no adverse effect on the hydration reaction of the alkali-activated slag, and to some extent, it helped to promote this reaction. In addition, some of the elements in the uranium tailings may have entered the structure of the hydration products via adsorption and exchange.

3.5 NMR Analysis of Hydration Products

Solid state nuclear magnetic resonance (NMR) can be used to analyze the polymerization degree of silica and alumina polyhedrons based on the position of the spectral line (chemical shift), which is useful in determining the structure of the substance. It is an effective means of analyzing the structures of the hydration products of cementitious materials. ^{29}Si and ^{27}Al are common nuclei with nuclear magnetic moments in cement-based materials (Fig. 8).

For the hydration products of AASP with a natural zeolite content of 0%, the ^{29}Si spectrum contains four peaks at −78.65, −86.412, −102.96 and −112.387 ppm, corresponding to Q^1 (chain tail) without hydration reaction in slag and Q^2, Q^4 (1Al), and Q^4 in the hydration products, respectively. The ^{27}Al spectrum contains two main peaks at 63.336 ppm and 5.296 ppm, indicating that the coordination of the ^{27}Al is both four and six but is mainly four coordination. According to Wang and Walkley, the relationship between the coordination = of ^{27}Al in the tetrahedron and its chemical shift is as follows: the Si at 75 ppm is Al instead of Si in C-S-H, resulting in C-A-S-H gels [33,34]. The ^{29}Si analysis revealed that Al was present instead of Si, which further indicates that the products of the alkali-activated slag cementitious material were C-(A)-S-H gels.

In the ^{29}Si spectrum of the hydration products of the AASP with a natural zeolite content of 16%, there are five peaks at −86.648, −97.606, −103.703, −107.212 and −110.08 ppm, corresponding to Q^2, Q^3, Q^4, Q^4 (1Al), and Q^4, respectively, but there is no obvious Q^1 unit, which indicates that the hydration reaction of the alkali-activated slag with a natural zeolite content of 16% was relatively sufficient. However, this may also be due to the chemical shift in the characterization of the Si in the natural zeolite minerals that were not involved in the reaction. The ^{27}Al spectrum mainly contains peaks at 62.984 ppm and 5.531 ppm, which is basically consistent with the characteristics when no natural zeolite was added.

It can be seen that the chemical environment of the AASP and the AASP mixed with natural zeolite was mainly Q^2, which is typical of C-(A)-S-H gel structures, and Q^3, Q^4, and Q^4 (1Al) have a high degree of polymerization, which is consistent with the results of the FTIR analysis.

When the natural zeolite content was 0%, compared with the AASP, the ^{29}Si NMR spectra of the hydration products screened from the CUTB had the following characteristics. First, there was a sharp characteristic peak at −112.873 ppm, which is an obvious characteristic of the ^{29}Si four coordination chemical shift, which corresponds to the Q^4 unit of a three-dimensional network structure with a higher degree of polymerization. Based on the ^{29}Si spectrum and FTIR spectrum of the AASP, this Q^4 unit does not represent a hydration product with a high degree of polymerization, and it was likely caused by the

SiO_2 in the uranium tailings mixed in during the sampling. Second, the characteristic peak shifted to the right (at −90.997 ppm) and became a broadener and smaller peak. The characteristic peak in the ^{27}Al spectrum also moved to the right. When the zeolite content was 16%, the variations in the ^{29}Si and ^{27}Al spectra were similar. It can be seen that the use of uranium tailings as the filler aggregate did not have an obvious effect on the hydration reaction of the alkali-activated slag cementitious material mixed with the functional minerals, and the CUTB had good chemical stability.

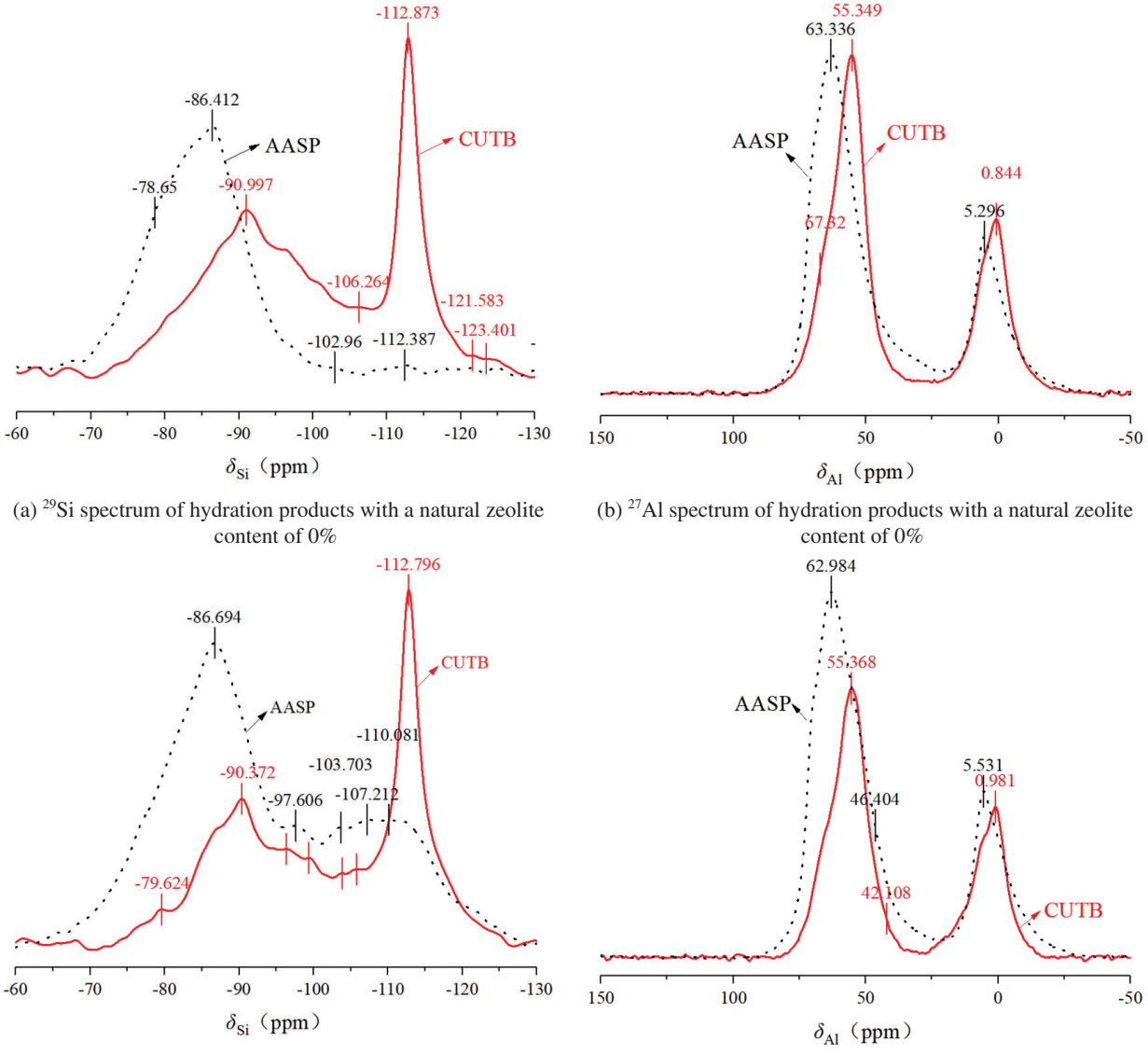

(a) ^{29}Si spectrum of hydration products with a natural zeolite content of 0%

(b) ^{27}Al spectrum of hydration products with a natural zeolite content of 0%

(c) ^{29}Si spectrum of hydration products with a natural zeolite content of 16%

(d) ^{27}Al spectrum of hydration products with a natural zeolite content of 16%

Figure 8: ^{29}Si and ^{27}Al spectra of hydration products

In conclusion, the influence of natural zeolite on the pore structure of CUTB is mainly due to its participation in the hydration reaction of alkali-activated slag, and the high degree of polymerization hydration products produced have different effects on different types of pore structures in CUTB (Fig. 9).

At the same time, the fluidity of filling slurry changes after adding natural zeolite, which inevitably affects the formation of various pore structures.

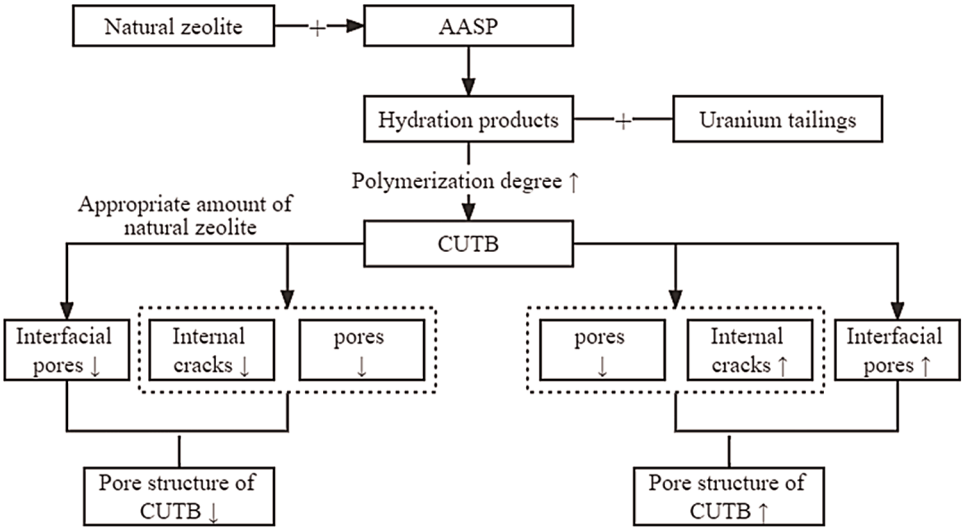

Figure 9: Influence of natural zeolite on the pore structure of CUTB

4 Conclusions

To study the influence of the addition of natural zeolite on the pore structure of the CUTB, the other conditions were fixed, the pore structure and UCS of the CUTB were tested, and the hydration products were analyzed. The conclusions that follow were drawn:

(1) When natural zeolite was added to the CUTB, the porosity generally increased to a certain extent, but the minimum porosity (only 22.30%) was reached at a content of 4%. This is because the addition of natural zeolite mainly reduced the number of fine pores in the CUTB. However, the pores with relaxation times T_2 of greater than 10 ms accounted for about 10% or more of the total pores, which also indicates that there are a certain number of large pores in the CUTB.

(2) The relationship between the UCS and porosity of the CUTB containing natural zeolite was nonlinear, and the function fitting degree was low, but it generally exhibited a negative correlation trend, that is, the greater the porosity, the smaller the UCS. This shows that in addition to the influence of the porosity, the mechanical properties of the CUTB were mainly affected by the hydration products of the alkali-activated slag mixed with the natural zeolite.

(3) The hydration products of the alkali-activated slag were mainly C-(A)-S-H gels. When natural zeolite was added, the hydration products became denser and had a high degree of polymerization; however, the reduction in the formation of low polymerization products led to the formation of larger fissure pores to a certain extent. This affected the flow properties of the slurry, thereby reducing the UCS of the CUTB.

(4) The pore structure of the CUTB included interfacial pores (between the filling aggregate and hydration products, the filling aggregate and filling aggregate, and the hydration products and hydration products) and internal cracks and pores in the hydration products. The particle size composition of the uranium tailings used as filling aggregate, the mixing of the slurry, the air bubbles generated during the pouring of the slurry into the molds, and the properties of the alkali-activated slag cementitious material all had significant effects on the generation of the interfacial pores.

(5) When natural zeolite was added to the CUTB as the backfill-modified material, its influence on the pore structure of the CUTB was complex, and the pore structure and mechanical properties affected and restricted each other. Therefore, it is not easy to draw a conclusion regarding the influence of its dosage on the pore structure and mechanical properties. It is necessary to investigate the influence of the change in the flow performance after its addition and the factors during the pouring of the slurry into the mold on the porosity.

Funding Statement: This research was funded by the National Natural Science Foundation of China (No. 51904154), Natural Science Foundation of Hunan Province (No. 2020JJ5491).

Conflicts of Interest: The authors declare that they have no conflicts of interest to report regarding the present study.

References

1. Vereshchagina, T., Kutikhina, E., Solovyov, L., Vereshchagin, S., Mazurova, E. et al. (2021). Hydrothermal co-processing of coal fly ash cenospheres and soluble Sr(II) as environmentally sustainable approach to Sr-90 immobilization in a mineral-like form. *Materials, 14(19)*. DOI 10.3390/ma14195586.
2. Li, J. F., Chen, L., Wang, J. L. (2021). Solidification of radioactive wastes by cement-based materials. *Progress in Nuclear Energy, 141,* 103957. DOI 10.1016/j.pnucene.2021.103957.
3. Wang, F. L., Chen, G. L., Ji, L., Yuan, Z. P. (2020). Preparation and mechanical properties of cemented uranium tailing backfill based on alkali-activated slag. *Advances in Materials Science and Engineering, 2020,* 6345206. DOI 10.1155/2020/6345206.
4. Mishra, D. P., Sahu, P., Panigrahi, D. C., Jha, V., Patnaik, R. L. (2014). Assessment of 222Rn emanation from ore body and backfill tailings in low-grade underground uranium mine. *Environmental Science and Pollution Research, 21(3),* 2305–2312. DOI 10.1007/s11356-013-2137-4.
5. Panigrahi, D. C., Mishra, D. P., Sahu, P. (2015). Evaluation of inhalation exposure contributed by backfill mill tailings in underground uranium mine. *Environmental Earth Sciences, 74(5),* 4327–4334. DOI 10.1007/s12665-015-4475-7.
6. Wang, F. L., Yuan, Z. P., Chen, G. L., Yang, S. J. (2020). Construction of uranium tailings underground filling disposal system with synergistic effect of paste and geopolymer. *Metal Mine, 2020(5),* 144–150 (in Chinese).
7. Jiang, F. L., Tan, B., Wang, Z., Liu, Y., Hao, Y. Y. et al. (2021). Preparation and related properties of geopolymer solidified uranium tailings bodies with various fibers and fiber content. *Environmental Science and Pollution Research, 29(14),* 20603–20616. DOI 10.1007/s11356-021-17176-0.
8. Chen, T., Li, J. W., Shi, P. H., Li, Y., Lei, J. et al. (2017). Effects of montmorillonite on the mineralization and cementing properties of microbiologically induced calcium carbonate. *Advances in Materials Science and Engineering*. DOI 10.1155/2017/7874251.
9. Deb, D., Sreenivas, T., Dey, G. K., Panchal, S. (2017). Paste backfill technology: Essential characteristics and assessment of its application for mill rejects of uranium ores. *Transactions of the Indian Institute of Metals, 70(2),* 487–495. DOI 10.1007/s12666-016-0999-0.
10. Panchal, S., Deb, D., Sreenivas, T. (2018). Mill tailings based composites as paste backfill in mines of U-bearing dolomitic limestone ore. *Journal of Rock Mechanics and Geotechnical Engineering, 10(2),* 310–322. DOI 10.1016/j.jrmge.2017.08.004.
11. Felipe-Sotelo, M., Hinchliff, J., Field, L. P., Milodowski, A. E., Preedy, O. et al. (2017). Retardation of uranium and thorium by a cementitious backfill developed for radioactive waste disposal. *Chemosphere, 179,* 127–138. DOI 10.1016/j.chemosphere.2017.03.109.
12. Kharchenko, G. V., Lenok, N. I. (2018). Technical-and-economic assessment of R&D efficiency in terms of uranium mining industry waste management. *Gornyi Zhurnal,* 12. DOI 10.17580/gzh.2018.12.08.

13. Zhang, S. Y., Ren, F. Y., Zhao, Y. L., Qiu, J. P., Guo, Z. B. (2021). The effect of stone waste on the properties of cemented paste backfill using alkali-activated slag as binder. *Construction and Building Materials, 283,* 122686. DOI 10.1016/j.conbuildmat.2021.122686.
14. Cihangir, F., Ercikdi, B., Kesimal, A., Deveci, H., Erdemir, F. (2015). Paste backfill of high-sulphide mill tailings using alkali-activated blast furnace slag: Effect of activator nature, concentration and slag properties. *Minerals Engineering, 83,* 117–127. DOI 10.1016/j.mineng.2015.08.022.
15. Cihangir, F., Akyol, Y. (2018). Mechanical, hydrological and microstructural assessment of the durability of cemented paste backfill containing alkali-activated slag. *International Journal of Mining Reclamation and Environment, 32(2),* 123–143. DOI 10.1080/17480930.2016.1242183.
16. Zhou, Q., Zhang, Y. Y., Liu, J. H., Wu, A. X., Wang, H. J. (2022). Research and application status and development trend of alkali-activated binder powder for mine backfill. *Journal of Renewable Materials, 10(12),* 3185–3199. DOI 10.32604/jrm.2022.020316.
17. Behera, S. K., Mishra, D. P., Singh, P., Mishra, K., Mandal, S. K. et al. (2021). Utilization of mill tailings, fly ash and slag as mine paste backfill material: Review and future perspective. *Construction and Building Materials, 309,* 125120. DOI 10.1016/j.conbuildmat.2021.125120.
18. Yu, R. C. (2020). *Theory and engineering practice of cemented backfill in metal mines*. Beijing, China: Metallurgical Industry Press.
19. Xu, W. B., Zhang, Y. L., Zuo, X. H., Hong, M. (2020). Time-dependent rheological and mechanical properties of silica fume modified cemented tailings backfill in low temperature environment. *Cement & Concrete Composites, 114*. DOI 10.1016/j.cemconcomp.2020.103804.
20. Chen, Q. S., Tao, Y. B., Feng, Y., Zhang, Q. L., Liu, Y. K. (2021). Utilization of modified copper slag activated by Na_2SO_4 and CaO for unclassified lead/zinc mine tailings based cemented paste backfill. *Journal of Environmental Management, 290*. DOI 10.1016/j.jenvman.2021.112608.
21. Tigue, A. A. S., Malenab, R. A. J., Dungca, J. R., Yu, D. E. C., Promentilla, M. A. B. (2018). Chemical stability and leaching behavior of one-part geopolymer from soil and coal fly ash mixtures. *Minerals, 8(9),* 411. DOI 10.3390/min8090411.
22. Benzaazoua, M., Fiset, J. F., Bussiere, B., Villeneuve, M., Plante, B. (2006). Sludge recycling within cemented paste backfill: Study of the mechanical and leachability properties. *Minerals Engineering, 19(5),* 420–432. DOI 10.1016/j.mineng.2005.09.055.
23. Barros, S. V. A., Dantas, G. C. B., Neves, G. D., Menezes, R. R. (2021). Immobilization of heavy metals present in quartzite residues through incorporation in mortars with total substitution of the natural aggregate. *Engenharia Sanitaria e Ambiental, 25(6),* 833–845. DOI 10.1590/S1413-4152202020180063.
24. Krajnak, A., Viglasova, E., Galambos, M., Krivosudsky, L. (2018). Kinetics, thermodynamics and isotherm parameters of uranium(VI) adsorption on natural and HDTMA-intercalated bentonite and zeolite. *Desalination and Water Treatment, 127,* 272–281. DOI 10.5004/dwt.2018.22762.
25. Jimenez-Reyes, M., Almazan-Sanchez, P. T., Solache-Rios, M. (2021). Radioactive waste treatments by using zeolites. A short review. *Journal of Environmental Radioactivity, 233,* 106610. DOI 10.1016/j.jenvrad. 2021.106610.
26. Saduakassova, A. T., Samoilov, V. I., Kulenova, N. A. (2016). Methods for sorption purification of underground water to remove uranium. *Russian Journal of Applied Chemistry, 89(4),* 583–589. DOI 10.1134/ S1070427216040108.
27. Gao, F. F., Tian, W., Cheng, X. (2021). Investigation of moisture migration of MWCNTs concrete after different heating-cooling process by LF-NMR. *Construction and Building Materials, 288,* 123146. DOI 10.1016/j. conbuildmat.2021.123146.
28. Zhang, P. F., Li, J. Q., Lu, S. F., Xue, H. T., Zhang, J. et al. (2017). A precise porosity measurement method for oil-bearing micro/nano porous shales using low-field nuclear magnetic resonance (LF-NMR). *Journal of Nanoscience and Nanotechnology, 17(9),* 6827–6835. DOI 10.1166/jnn.2017.14518.
29. Shi, C. J., Yuan, Q. (2018). *Test and analysis methods of cement-based material*. Beijing, China: Architecture & Building Press.

30. Deng, Z. Z., Zhou, W., Yue, H., Guo, X. Y. (2019). Study on the hydration mechanism of a hardened slag-based plugging agent activated by alkalis. *Construction and Building Materials, 203*, 343–355. DOI 10.1016/j.conbuildmat.2019.01.015.
31. Lei, J. W., Law, W. W., Yang, E. H. (2021). Effect of calcium hydroxide on the alkali-silica reaction of alkali-activated slag mortars activated by sodium hydroxide. *Construction and Building Materials, 272,* 121868. DOI 10.1016/j.conbuildmat.2020.121868.
32. Adesanya, E., Ohenoja, K., di Maria, A., Kinnunen, P., Illikainen, M. (2020). Alternative alkali-activator from steel-making waste for one-part alkali-activated slag. *Journal of Cleaner Production, 274,* 123020. DOI 10.1016/j.jclepro.2020.123020.
33. Wang, K., Zhang, Y. H., Li, Y. Q., Zou, D. H. (2020). Applications of solid-state nuclear magnetic resonance spectroscopy in cementitious materials research. *Chinese Journal of Magnetic Resonance, 37(1),* 40–51 (in Chinese).
34. Walkley, B., Provis, J. L. (2019). Solid-state nuclear magnetic resonance spectroscopy of cements. *Materials Today Advances, 1,* 100007. DOI 10.1016/j.mtadv.2019.100007.